

ORIENTATION OF QUICKBIRD, IKONOS AND EROS A STEREOPAIRS BY AN ORIGINAL RIGOROUS MODEL

M. Crespi, F. Fratarcangeli, F. Giannone, F. Pieralice

DITS, Area di Geodesia e Geomatica, Sapienza Università di Roma, via Eudossiana 18, 00184 Rome, Italy
(mattia.crespi, francesca.fratarcangeli, francesca.giannone, francesca.pieralice)@uniroma1.it

KEY WORDS: Pushbroom sensors, HRSI stereopairs, rigorous models, software

ABSTRACT:

Interest in high-resolution stereopairs satellite imagery (HRSI) is spreading in several application fields, mainly for the generation of Digital Elevation and Digital Surface Models (DEM/DSM) and for 3D feature extraction (e.g. for city modeling). The satellite images are possible alternative to aerial photogrammetric, especially in areas where the organization of photogrammetric surveys may result critical. However, the real possibility of using HRSI for 3D applications strictly depends on their orientation, whose accuracy is related on the imagery quality (noise and radiometry), on the Ground Control Points (often obtained by GPS surveys) quality, and on the model chosen to perform the orientation.

Since 2003, the research group at the Area di Geodesia e Geomatica - Sapienza Università di Roma has been developing a specific and rigorous model designed for the orientation of single and stereo imagery acquired by pushbroom sensors carried on satellite platforms. This model has been implemented in the software SISAR (Software Immagini Satellitari Alta Risoluzione).

In this paper the attention is focused on the orientation of QuickBird, IKONOS and EROS A stereopairs. In the first version the model was able to manage along-track imagery acquired with a time delay in the order of seconds only; anyway, the cost of stereo data is usually very high, so that it became interesting to investigate which is the quality of the geometric information which can be extracted from stereopairs formed by imagery collected on different tracks and dates.

The SISAR model is tested on QuickBird, EROS A and IKONOS images with different features; to point out the effectiveness of the new model, SISAR results are compared with the corresponding ones obtained by the software OrthoEngine 10.0 (PCI Geomatica), where Thierry Toutin's rigorous model for the imagery elaboration of the main high-resolution sensors is implemented.

1 INTRODUCTION

The real possibility of using High Resolution satellite Imagery (HRSI) for cartography depends on several factors: sensor characteristics (geometric and radiometric resolution and quality), types of products made available by the companies managing the satellites, cost and time needed to actually obtain these products, cost of the software suited for the final processing to realize the cartographic products.

The first and fundamental task to be addressed is the imagery distortions correction, that is the so called orientation and orthorectification.

The distortions sources can be related to two general categories: the acquisition system, including the platform orientation and movement and the imaging sensor optical-geometric characteristics, and the observed object, accounting for the atmosphere refraction and terrain morphology.

At present, HRSI orientation methods can be classified in three categories: black models (like Rational Polynomial Function - RPF), consisting in purely analytic functions linking image to terrain coordinates, independently of specific platform or sensor characteristics and acquisition geometry; physically based models (so called "rigorous models"), which take into account several aspects influencing the acquisition procedure and are often specialized to each specific platform and sensor; the gray models (like Rational Polynomial Coefficients - RPC models), in which the mentioned RPF are used with known coefficients supplied in the imagery metadata and "blind" produced by companies managing sensors by their own secret rigorous models.

In this paper the attention is focused on an original rigorous model suited for the orientation of stereopairs acquired by QuickBird, IKONOS and EROS A platforms. For QuickBird and EROS A Basic imagery are concerned, whereas for IKONOS Geo Ortho Kit imagery are considered.

The model, implemented into the SISAR software, is able to manage along-track imagery acquired with a time delay in the order of seconds and also a couple of image formed by imagery collected on different tracks and dates. This last features is very important because satellite imagery pairs collected during different orbital passages are often already available in large archive mainly focused on populated and urban areas and their cost are remarkably lower if compared to those of along-track stereopairs.

The models for QuickBird - EROS A and IKONOS are briefly described in section §2 and §3; in §4 the strategy for Tie Point approximate coordinate computation is illustrated. Finally, in §5 the results of SISAR and OrthoEngine and their comparison are presented and discussed.

Since 2003, the research group at the Area di Geodesia e Geomatica - Sapienza Università di Roma has developed specific and rigorous models designed for the orientation of imagery acquired by pushbroom sensors carried on satellite platforms, like EROS-A, QuickBird and IKONOS. These models have been implemented in the software SISAR.

The first version of the model (Crespi et al., 2003) was uniquely focused on EROS-A imagery, since no commercial software including a rigorous model for this platform were available at that time. Later, the model was refined (Baiocchi et al., 2004) and extended to process QuickBird Basic imagery too and, at present (since January 2007), the software was extended to IKONOS imagery (Crespi et al., 2007). The RPC (use and generation) and rigorous orientation of stereo pairs models are now under implementation and the first results are encouraging (Table 1).

The rigorous models implemented in SISAR are based on a standard photogrammetric approach describing the physical-geometrical imagery acquisition. Of course, in this case, it has to be considered that an image stemming from a pushbroom sensor is formed by many (from thousands to tens of thousands) lines, each acquired with a proper position (projection center) and attitude.

SENSOR	SINGLE IMAGE		STEREO PAIRS
	Rigorous	RPC (use/generation)	Rigorous
EROS A	YES	YES	YES
QuickBird Basic	YES	YES	YES
IKONOS II	YES	U.I.*	YES
QuickBird Standard Orthoready	U.I.	U.I.	U.I.

Table 1: SISAR software present facilities (*U.I.=Under Implementation)

All the acquisition positions are related by the orbital dynamics. Therefore, rigorous models implemented in SISAR are based on the collinearity equations, with the reconstruction of the orbital segment during the image acquisition through the knowledge of the acquisition mode, the sensor parameters, the satellite position and attitude parameters.

The approximate values of these parameters can be computed thanks to the information contained in the metadata file delivered with each image; these approximate values must be corrected by a least squares (LS) estimation process based on a suitable number of Ground Control Points (GCPs). Also the GCP coordinates are treated as pseudo-observations and may be refined within the LS estimation process.

Nevertheless, due to the intrinsic differences between Basic and Geo Ortho Kit imagery, the structures of rigorous models for QuickBird and EROS A (on one side) and for IKONOS (on the other one) are remarkably different and will be described separately. As a matter of fact it is well known that Basic imagery are radiometrically corrected and sensor corrected, but not geometrically corrected nor mapped to a cartographic projection and ellipsoid (DigitalGlobe, 2006); whereas Geo Ortho Kit imagery are map projected, rectified to a datum and map projection system and then they are resampled to a uniform ground sample distance (GSD) and a specified map projection (GeoEye, 2006).

2 EROS A AND QUICKBIRD BASIC IMAGERY STEREOPAIRS ORIENTATION

2.1 Coordinate systems

The collinearity equations relate the image to the ground coordinates, expressed in an Earth Centered - Earth Fixed (ECEF) reference frame, through a set of rotation matrices. These matrices include those needed to shift between sensor, body, flight and Earth Centered Inertial (ECI) coordinate systems, while the transformation between ECI and ECEF coordinate systems must take into account precession, nutation, polar motion and Earth rotation matrices (Kaula, 1966).

Therefore, in order to describe the collinearity equations, the definitions of some coordinate systems are needed:

Image system (I): is a 2-dimensional system describing a point position in an image. The origin is in the upper left corner, the pixel position is defined by its row (J) and column (I). The column numbers increases toward the right and row numbers increases in the downward direction.

Sensor system (S): the origin is in the perspective center, the x-axis is tangent to the orbit directed as the satellite motion, the z-axis is directed from the perspective center to pixel array and y-axis is parallel to pixel array.

Body system (B): it is aligned to the Flight system (see below) when the angle Roll (φ), Pitch (θ) and Yaw (ψ) are zero.

Flight system (F): the origin is in the perspective center, the X-axis is tangent to the orbit along the satellite motion, the Z-axis is in the orbital plane directed toward the Earth center of mass and the Y-axis completes the right-handed coordinate system.

Earth Centered Inertial system - ECI (I): the origin is in the Earth center of mass, the X-axis points to vernal equinox (epoch J2000 - 1 January 2000, ore 12 UT), the Z-axis points to celestial north pole (epoch J2000) and the Y-axis completes the right-handed coordinate system.

Earth-Centered Earth-Fixed system - ECEF (E): the origin is in the Earth center of mass, the X-axis is the intersection of equatorial plane and the plane of reference meridian (epoch 1984.0), the Z-axis is the mean rotational axis (epoch 1984.0) and the Y-axis completes the right-handed coordinate system.

The transformation matrix from the sensor systems to the ECI one can be expressed through three rotations (Westin, 1990)

$$R_{SI} = R_{FI} \cdot R_{BF} \cdot R_{SB} \quad (1)$$

Inertial-Flight matrix (R_{FI}): it allows the passage from the inertial geocentric system (ECI) to the orbital one; it is a function of keplerian orbital parameters and varies with the time inside each scene (for each image row J)

$$R_{FI} = [R_x(-\pi/2) \cdot R_z(\pi/2)] \cdot [R_z(U) \cdot R_x(i) \cdot R_z(\Omega)] \quad (2)$$

where i is the inclination, Ω the right ascension of the ascending node, $U = \omega + v$ with ω argument of the perigee and v true anomaly.

Flight-Body matrix (R_{BF}): it allows the passage from the orbital system to the body one through the attitude angles (φ , θ , ψ) which depend on time (for each pixel row)

$$R_{BF} = R_z(\psi) \cdot R_y(\theta) \cdot R_x(\varphi) \quad (3)$$

Body-Sensor matrix (R_{SB}): it allows the passage from the body to the sensor system. This matrix considers defect of parallelism between axes $(X, Y, Z)_S$ and $(X, Y, Z)_B$ and it is considered constant during a scene for each sensor; the elements of the matrix are usually provided in the metadata files.

The product of R_{EI} and R_{SI}^T matrices allows the passage from sensor S to ECEF system, the final rotation matrix being:

$$R_{ES} = R_{EI} \cdot R_{SI}^T = R_z(K) \cdot R_y(P) \cdot R_x(W) \quad (4)$$

the angles (K , P , W) define the satellite attitude at the moment of the acquisition of image row J with respect to the ECEF system.

The rotation matrix for the transformation from ECI system to ECEF system (R_{EI}) can be subdivided into four different steps, considering the motions of the Earth in the space: precession, the secular change in the orientation of the Earth's rotation axis and the vernal equinox (described by the matrix R_P); nutation, the periodic and short-term variation of the equator and the vernal equinox (described by the matrix R_N); polar motion, the coordinates of the rotation axis relative to the IERS Reference Pole (described by the matrix R_M) and Earth's rotation about its axis (described by the Sideral Time through the matrix R_S) (Montenbruck and Gill, 2001).

$$R_{EI} = R_M \cdot R_S \cdot R_N \cdot R_P \quad (5)$$

2.2 Model definition

As mentioned, the rigorous model for QuickBird and EROS A platforms bases the imagery orientation on the well known collinearity equations, including different subsets of parameters (Table 2) for the satellite position, the sensor attitude and the viewing geometry (internal orientation and self-calibration).

In particular, the satellite position is described through the Keplerian orbital elements attaining to the orbital segment during the image acquisition; the sensor attitude is supposed to be represented by a known time-dependent term plus a 2nd order time-dependent polynomial, one for each attitude angle; moreover, atmospheric refraction is accounted for by a general model for remote sensing applications (Noerdlinger, 1999). The viewing geometry is supposed to be modeled by the focal length and five self-calibration parameters, able to account for a second order distortion along the array of detectors direction (see Equation 7).

SATELLITE POSITION	a : semi-major axis e : eccentricity Ω : right ascension of the ascending node i : orbit inclination ω : argument of the perigee v : true anomaly (dependent on T_P , the time of the passage at perigee)
SENSOR ATTITUDE	$\varphi = \tilde{\varphi} + a_0 + a_1\tau + a_2\tau^2$ $\vartheta = \tilde{\vartheta} + b_0 + b_1\tau + b_2\tau^2$ $\psi = \tilde{\psi} + c_0 + c_1\tau + c_2\tau^2$
VIEWING GEOMETRY	f : focal length I_0, J_0, K, d_1, d_2 : self calibration

Table 2: Full parametrization of the SISAR model

So, for the stereopair orientation, the set of parameters is constituted by the Keplerian parameters, one internal parameter (the focal length), five self calibration parameters and 18 attitude coefficients (9 for each image).

It is now possible to write the collinearity equations in an explicit form for a generic ground point

$$x_s = f \frac{R_1 |X_{tI} - X_{sI}|}{R_3 |X_{tI} - X_{sI}|} \quad y_s = f \frac{R_2 |X_{tI} - X_{sI}|}{R_3 |X_{tI} - X_{sI}|} \quad (6)$$

where (x_s, y_s) are the image coordinates (in metric units), f is the focal length, R_1, R_2, R_3 are the rows of the total rotation matrix $R = R_{SB} R_{BF} R_{FI}$ and (X_{tI}, X_{sI}) are the ground point and the satellite positions in ECI system.

With simple geometric considerations (Figure 1) it is possible to write the collinearity equations as functions of the image coordinates (I, J) (in pixels):

$$\begin{cases} \frac{x_s}{f} = \tan \beta = \frac{d_{pix}}{f} [J - \text{int}(J) - 0.5 - J_0 - k(I - I_0)] \\ \frac{y_s}{f} = -\tan \alpha = -\frac{d_{pix}}{f} \left\{ d_1(I - I_0) + d_2(I - I_0)^2 + k[J - \text{int}(J) - 0.5 - J_0] \right\} \end{cases} \quad (7)$$

where d_{pix} is the image pixel dimension and (I_0, J_0) are the principal point coordinates (in pixels).

Substituting equations (7) into equations (6) the collinearity equations become:

$$\begin{cases} R_1 |X_{tI} - X_{sI}| - \left\{ \frac{d_{pix}}{f} [J - \text{int}(J) - 0.5 - J_0 + k(I - I_0)] \right\} R_3 |X_{tI} - X_{sI}| = 0 \\ R_2 |X_{tI} - X_{sI}| + \frac{d_{pix}}{f} \left\{ d_1(I - I_0) + d_2(I - I_0)^2 + k[J - \text{int}(J) - 0.5 - J_0] \right\} R_3 |X_{tI} - X_{sI}| = 0 \end{cases} \quad (8)$$

these equations are linearized with respect to both the parameters aforementioned and to the image and ground coordinates (Teunissen, 2001).

The collinearity equations are a function of the parameters described in Table 2. The approximate values for all parameters may be derived from the information contained into the metadata

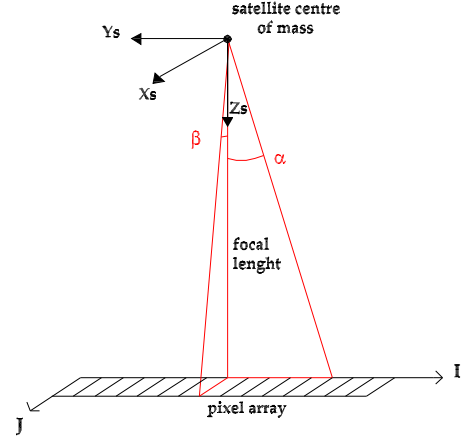


Figure 1: Sensor (S) and Image (I) coordinate systems

files released together with the imagery or they are simply fixed to zero. In theory, these approximate values must be corrected by an estimation process based on a suitable number of Ground Control Points (GCPs), for which the collinearity equations are written; nevertheless, since the orbital arc related to each image acquisition is extremely short (few hundreds of kilometers) if compared to the whole orbit length (tens of thousandths), some Keplerian parameters are not estimable at all (a, e, ω) and others ($i, \Omega, T_p, I_0, J_0, k$) are usually extremely correlated both among them and with sensor attitude and viewing geometry parameters (Giannone, 2006).

In order to avoid instability due to high correlations among some parameters leading to design matrix pseudo-singularity, Singular Value Decomposition (SVD) and QR decomposition are employed to evaluate the actual rank of the design matrix, to select the estimable parameters and finally to solve the linearized collinearity equations system in the LS sense (Golub and Van Loan, 1993) (Strang and Borre, 1997) (Press et al., 1992).

3 IKONOS GEO ORTHO KIT IMAGERY STEREOPAIRS ORIENTATION

The IKONOS rigorous model is also based on the collinearity equations, but this model displays several differences in respect to the EROS-A and QuickBird models, because of many reasons. The first one is that Space Imaging does not release camera model (calibration data) and precise ephemeris data for the satellite.

The second reason is that IKONOS Geo Ortho Kit imagery are pre-processed, in particular they are map projected to a datum (ellipsoid at the mean elevation of the covered area) and map projection system; they also undergo a correction process to remove image distortions and to resample it to a uniform Ground Sampling Distance (GSD).

So, the collinearity equations relate the points in the object space with the points projected on the "inflated" ellipsoid, on the contrary the classical photogrammetric collinearity equations establish a relation between the object space and the image plane.

IKONOS Geo Ortho Kit imagery are georeferenced at the level of tens of meters and it is possible to compute cartographic coordinate for each image point with the following relations:

$$\begin{cases} N_I = N_A - J \cdot p \\ E_I = E_A - I \cdot p \end{cases} \quad (9)$$

where N_A, E_A are the upper left corner coordinates of the image (available on metadata file), p is the GSD (available on metadata

file). The ellipsoidal height of the points on the image is the elevation of "inflated" ellipsoid; this parameter is contained in metadata file and is called reference height.

The cartographic coordinates are converted in geographic coordinates (latitude and longitude), and then they are transformed in ECEF coordinates (X_I, Y_I, Z_I).

The image coordinate are written in collinearity equations, that are directly expressed in ECEF system.

$$\begin{vmatrix} X_I - X_S \\ Y_I - Y_S \\ Z_I - Z_S \end{vmatrix} = \lambda R \begin{vmatrix} X_T - X_S \\ Y_T - Y_S \\ Z_T - Z_S \end{vmatrix} \Rightarrow \begin{cases} \frac{X_I - X_S}{Z_I - Z_S} = \frac{R_1 |X_T - X_S|}{R_3 |Z_T - Z_S|} \\ \frac{Y_I - Y_S}{Z_I - Z_S} = \frac{R_2 |Y_T - Y_S|}{R_3 |Z_T - Z_S|} \end{cases} \quad (10)$$

The other terms in the equations are: the satellite coordinates (X_S, Y_S, Z_S), the ground coordinates (X_T, Y_T, Z_T), a scale factor (λ) and the rows of a rotation matrix (R_1, R_2, R_3). The rotation matrix R is linearized because it represents an infinitesimal rotation around the satellite position, since the direct georeferencing is at the level of tens of meters. So R matrix can be expressed as sum of identity matrix and an antisymmetric matrix.

$$R = I + \delta R \quad \delta R = \begin{bmatrix} 0 & a & b \\ -a & 0 & c \\ -b & -c & 0 \end{bmatrix} \quad (11)$$

$$R = \begin{bmatrix} 1 & a & b \\ -a & 1 & c \\ -b & -c & 1 \end{bmatrix}$$

The satellite attitude can change during the image acquisition, and it is supposed to be modeled by a time-dependent function at the second order. In the following functions can be used the J_s variable, that represents the scanning row and it is equivalent to the time variable.

$$\begin{cases} a = a_0 + a_1 \cdot J_s + a_2 \cdot J_s^2 \\ b = b_0 + b_1 \cdot J_s + b_2 \cdot J_s^2 \\ c = c_0 + c_1 \cdot J_s + c_2 \cdot J_s^2 \end{cases} \quad (12)$$

Thus the parameters that can be estimated are 9 ($a_0, b_0, c_0, a_1, b_1, c_1, a_2, b_2, c_2$) for each image (for the stereopair orientation the attitude parameters are 18).

Two angles available in the metadata file, the *nominal collection elevation* and the *nominal collection azimuth* (Figure 2) allow to calculate an approximated satellite position referred to the centre of the image.

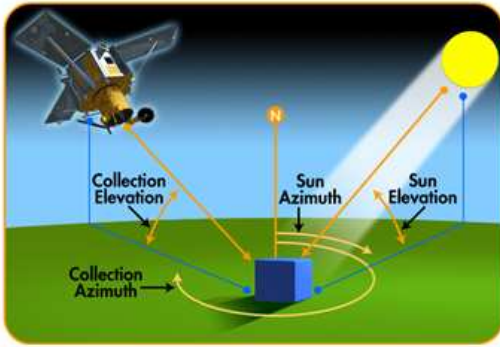


Figure 2: Information about IKONOS acquisition (Courtesy of Dr. Tine Flingelli - European Space Imaging)

Then the satellite coordinates can be refined calculating one position for each GCP taking into consideration the approximate information about IKONOS orbit (always descendent, with an inclination angle of about 98.2°) and acquisition mode (*forward or reverse scan and scan azimuth*), these last data being included into the metadata file.

Model computation is complete when the unknowns ($a_0, b_0, c_0, a_1, b_1, c_1, a_2, b_2, c_2$) are estimated.

The values of the nine parameters of the matrix rotation can be assessed by an estimation process based on a suitable number of Ground Control Points (GCPs), for which collinearity equations are written; the approximate value for the unknowns is zero.

4 TIE POINT GROUND COORDINATES

In the SISAR module devoted to stereopairs orientation an algorithm to compute approximate Tie Point (TP) ground coordinates was implemented, taking advantage from a simplified geometry after the separate orientation of the two images (Figure 3)(Corsetti et al., 2007). For each TP two sets of ground coordinates ($(X, Y, Z)_1$ and $(X, Y, Z)_2$) can be computed through the intersection of collinearity equations (r for the image 1, s for the image 2) with WGS 84 ellipsoid; then TP ground coordinates are computed with the following procedure.

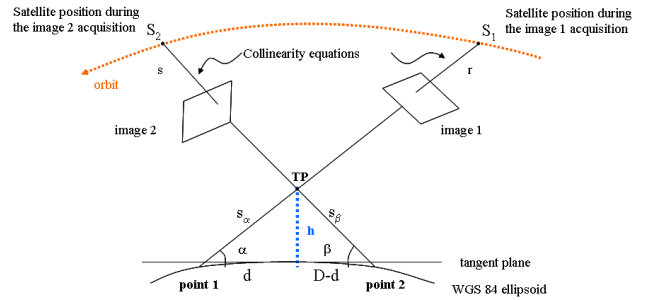


Figure 3: Tie Point approximate ground coordinates computation

The two vectors \vec{s}_α and \vec{s}_β are calculated:

$$\vec{s}_\alpha = \frac{h}{\sin \alpha} \begin{vmatrix} \cos(X_1 X_{S1}) \\ \cos(Y_1 Y_{S1}) \\ \cos(Z_1 Z_{S1}) \end{vmatrix} = \frac{D \cdot tg \beta}{\cos \alpha \cdot (tg \alpha + tg \beta)} \begin{vmatrix} \cos(X_1 X_{S1}) \\ \cos(Y_1 Y_{S1}) \\ \cos(Z_1 Z_{S1}) \end{vmatrix}$$

$$\vec{s}_\beta = \frac{h}{\sin \beta} \begin{vmatrix} \cos(X_2 X_{S2}) \\ \cos(Y_2 Y_{S2}) \\ \cos(Z_2 Z_{S2}) \end{vmatrix} = \frac{D \cdot tg \alpha}{\cos \beta \cdot (tg \alpha + tg \beta)} \begin{vmatrix} \cos(X_2 X_{S2}) \\ \cos(Y_2 Y_{S2}) \\ \cos(Z_2 Z_{S2}) \end{vmatrix} \quad (13)$$

where D is the distance between the coordinates of points 1 and 2, and α and β are the angles between the collinearity equations and tangent plane to WGS 84 ellipsoid. Then ground coordinates $(X, Y, Z)_1$ and $(X, Y, Z)_2$ are increased of \vec{s}_α and \vec{s}_β respectively. The final TP coordinates are obtained as the average between the two sets previous described.

The GP coordinates (GCP and TP) are then refined in a least squares process.

5 RESULTS

The SISAR models were tested on QuickBird and EROS A and IKONOS images with different features. In particular, the QuickBird Basic stereopair was acquired over the zone of Augusta (Sicily) during the same orbital passage; the EROS A images, level

1A, consist in two scenes over the same area of Rome with different extension but completely overlapped, acquired with a temporal shift of about 1 year; the two IKONOS stereopairs are partially overlapped (so forming a small block) and were acquired over the zone of Bagnoli (Naples).

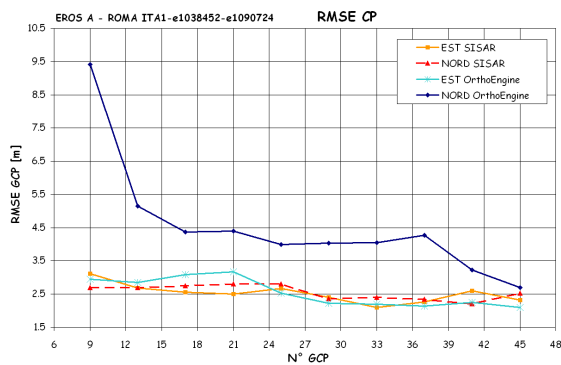
The imagery acquired by the platforms EROS A and QuickBird have only radiometric corrections, while the IKONOS II stereopair are pre-processed (for the features of all images see Table 3).

Area	GSD [m]	Off-nadir angle (°)		Scene coverage (Km×Km)	GP
		start	end		
EROS A					
ITA1-e1038452 (Rome)	1.80	9.1	9.4	13×10	49
ITA1-e1090724 (Rome)	2.60	31.0	40.1	17×12	
QuickBird					
Augusta (*P001)	0.77	29.2 (mean value)		20×19	39
Augusta (*P002)	0.75	28.2 (mean value)		20×19	
IKONOS					
Bagnoli 1	1.00	25.6 (mean value)		9×13	25
Bagnoli 2	1.00	27.1 (mean value)		9×13	

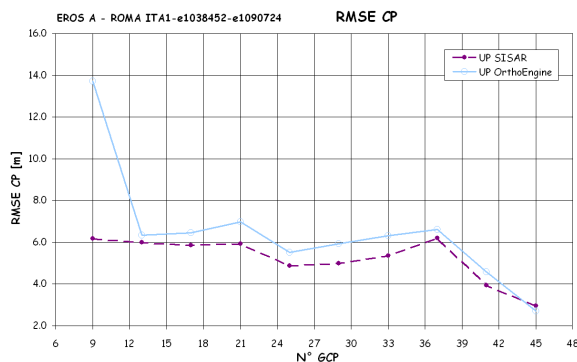
Table 3: Test images

5.1 EROS A results

The accuracies for the Eros A images are respectively at the level of 2.6 m (North) and 2.5 m (East) for SISAR and at the level of 4.6 m (North) and 2.6 m (East) for OrthoEngine. So, specially in North component SISAR achieves better accuracy than OrthoEngine (Figure 4(a)).



(a) North an East components



(b) Up component

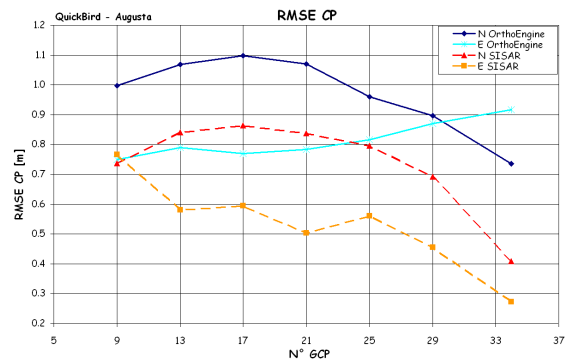
Figure 4: RMSE CP trend for EROS A stereopair

The GSD values for the two images are 1.8 m and 2.6 m, thus the results are satisfactory since the accuracy is comparable with the GSD value.

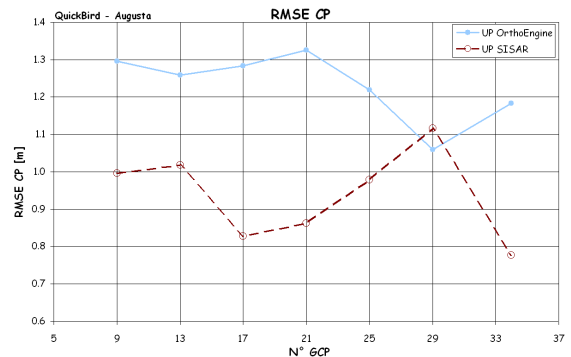
For the Up component the trend of the RMSE on CPs is similar for the two software, but SISAR accuracy is around 5 m and OrthoEngine one is around 6.5 m (Figure 4(b)).

5.2 QuickBird results

In the North component the RMSE CP trend is similar, although SISAR has the best accuracy; on the contrary in the East component the CP trend is different for the two software and SISAR shows again better results with respect to OrthoEngine (Figure 5(a)).



(a) North an East components



(b) Up component

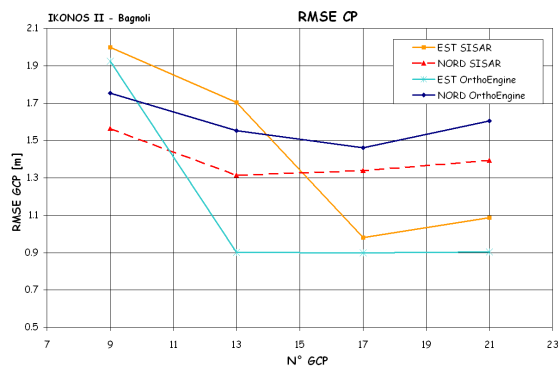
Figure 5: RMSE CP trend for QuickBird stereopair

In Up component the CP trend has a different value range for two software; for SISAR the accuracy varies between 0.8 and 1.1 m, instead for OrthoEngine it varies between 1.2 and 1.3 m (Figure 5(b)).

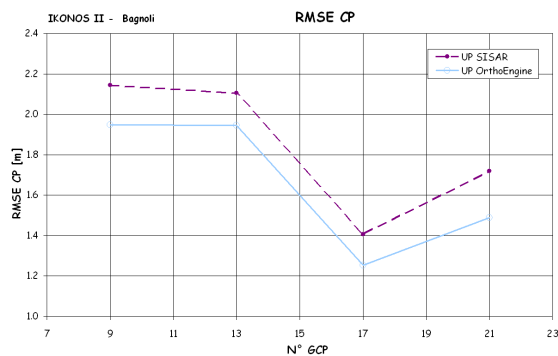
5.3 IKONOS results

For the IKONOS Geo Ortho Kit stereopairs, the following graphics show a similar trend for both software, specially on the North component. In particular on the North component SISAR results are better than OrthoEngine ones, whereas the opposite is true for the East component (Figure 6(a)).

In the Up component the accuracy trend is the same for both software; for SISAR the accuracy varies between 1.4 m and 2.1 m, instead for OrthoEngine it varies between 1.2 m and 2.0 m (Figure 6(b)).



(a) North and East components



(b) Up component

Figure 6: RMSE CP trend for IKONOS II stereopair

6 CONCLUSIONS AND FUTURE WORK

Original rigorous models for the orientation of Basic imagery (level 1A) collected by EROS A and QuickBird and pre-processed IKONOS Geo Ortho Kit imagery (level 1B) were developed and implemented into the software SISAR at the Area di Geodesia e Geomatica - Sapienza Università di Roma.

To point out the effectiveness of the new models, SISAR results were compared with the corresponding ones obtained by the well known software OrthoEngine (PCI Geomatica) v. 10.0, where Thierry Toutin's rigorous models for the imagery orientation of the main HRSI are implemented.

In details, three couples of images were concerned, showing that SISAR performs at the level and sometime better than OrthoEngine.

Results stemming from the elaborations of QuickBird imagery show that accuracy at sub-meter level, compatible with cartographic product at 1:5000 scale, is achievable.

Instead, for the IKONOS and EROS A imagery the metric values of RMSE on CPs are worse than QuickBird ones, but however achievable accuracy is comparable with their GSD, therefore the SISAR results are very encouraging.

Future prospects regard the rigorous model extension to Cartosat-1 and Prism satellites.

ACKNOWLEDGEMENTS

This research was supported by grants of the Italian Ministry for School, University and Scientific Research (MIUR) in the frame of the project: MIUR-COFIN 2005 - "Analisi, comparazione e integrazione di immagini digitali acquisite da piattaforma aerea e satellitare" - National Principal Investigator: S. Dequal.

The Authors thank very much Informatica Per il Territorio - Rome, Italy, Eurimage - Rome, Italy, Sysdeco Italia - Rome, Italy for supplying the stereopairs used in this investigation.

REFERENCES

Baiocchi, V., Crespi, M., Vendictis, L. D. and Giannone, F., 2004. A new rigorous model for the orthorectification of synchronous and asynchronous high resolution imagery. Proceedings of the 24th EARSeL Symposium, Dubrovnik (Croatia) pp. 461–468.

Corsetti, M., Crespi, M., Fratarcangeli, F. and Giannone, F., 2007. A rigorous model for asynchronous high resolution satellite sensors. 27th EARSeL Symposium, Bolzano (Italy).

Crespi, M., Baiocchi, V., Vendictis, L. D., Lorenzon, F., Mezzapesa, M. and Tius, E., 2003. A new method to orthorectify eros a1 imagery. Proc. of 2003 Tyrrhenian International Workshop on Remote Sensing pp. 566–575.

Crespi, M., Fratarcangeli, F., Giannone, F. and Pieralice, F., 2007. Sisar: a rigorous orientation model for synchronous and asynchronous pushbroom sensors imagery. ISPRS Commission I, WG I/V Meeting, Hannover.

DigitalGlobe, 2006. Quikbird imagery products guide. Available online at: http://www.digitalglobe.com/product/product_docs.shtml.

GeoEye, 2006. Ikonos imagery products guide. Available online at: <http://www.geoeye.com/products/imagery/ikonos/default.htm>.

Giannone, F., 2006. A rigorous model for High Resolution Satellite Imagery Orientation. PhD Thesis, Area di Geodesia e Geomatica Dipartimento di Idraulica Trasporti e Strade, Sapienza Università di Roma. Available online at: [http://w3.uniroma1.it/geodgeom/geodgeomrw/downloads/tesi%20dottorato/PhD%](http://w3.uniroma1.it/geodgeom/geodgeomrw/downloads/tesi%20dottorato/PhD%20)

Golub, G. and Van Loan, C. F., 1993. Matrix computation. The Johns Hopkins University Press, Baltimore and London.

Kaula, W. M., 1966. Theory of Satellite Geodesy. Blaisdell Publishing Company.

Montenbruck, O. and Gill, E., 2001. Satellite orbits. Springer, Berlin.

Noerdlinger, P. D., 1999. Atmospheric refraction effects in earth remote sensing. ISPRS Journal of Photogrammetry & Remote Sensing 54, pp. 360–373.

Press, W. H., Teukolsky, S. A., Vetterling, W. and Flannery, B., 1992. Numerical recipes in c: The art of scientific computing. Cambridge University Press (ISBN 0-521-43108-5). <http://www.nr.com> (accessed on April 10, 2006).

Strang, G. and Borre, K., 1997. Linear algebra, geodesy and gps. Wellesley-Cambridge Press, Wellesley.

Teunissen, P. J. G., 2001. Adjustment theory. series on mathematical geodesy and positioning. Delft University Press.

Westin, T., 1990. Precision rectification of spot imagery. Photogrammetric Engineering and Remote Sensing 56, pp. 247–253.